

Received 1 February 2023, accepted 15 February 2023, date of publication 20 February 2023, date of current version 21 March 2023.

Digital Object Identifier 10.1109/ACCESS.2023.3246512

## RESEARCH ARTICLE

# Causal Signal Temporal Logic for the Environmental Control and Life Support System's Fault Analysis and Explanation

ZIQUAN DENG<sup>1</sup>, (Graduate Student Member, IEEE), SAMUEL P. ESHIMA<sup>2</sup>, JAMES NABITY<sup>2</sup>, AND ZHAODAN KONG<sup>1</sup>, (Member, IEEE)

<sup>1</sup>Department of Mechanical and Aerospace Engineering, University of California at Davis, Davis, CA 95616, USA

<sup>2</sup>Department of Smead Aerospace Engineering Sciences, University of Colorado, Boulder, CO 80303, USA

Corresponding author: Zhaodan Kong (zdkong@ucdavis.edu)


This work was supported by the National Aeronautics and Space Administration's Space Technology Research Grants Program (grant number 80NSSC19K1052).

**ABSTRACT** Modern cyber-physical systems would often fall victim to unanticipated anomalies. Humans are still required in many operations to troubleshoot and respond to such anomalies, such those in future deep space habitats. To maximize the effectiveness and efficiency of the anomaly response process, the information provided by anomaly response technologies to their human operators must be epistemically accessible or explainable. This paper offers a first step towards developing explainable anomaly response systems. It proposes a logic, Causal Signal Temporal Logic (CaSTL), which can formally describe cause-effect relationships pertaining to fault explanation. Moreover, it develops an algorithm to infer a CaSTL formula that explains why a fault has happened in a system, given the model of the system and an observation about the fault. The effectiveness of the proposed algorithm is demonstrated with a simulated Environmental Control and Life Support System (ECLSS).

**INDEX TERMS** Explanation, diagnostic reasoning, failure analysis, simulation, temporal logic, troubleshooting.

## I. INTRODUCTION

Modern cyber-physical systems (CPSs) are becoming increasingly complex and being deployed in more safety-critical missions such as transportation, health care, manufacturing, aerospace, and defense [1], [2]. Since the concept of CPS was first proposed in [3], its intent has been constantly expanded by a series of works [4], [5], [6]. One notable characteristic is the increasing attention paid to the role of humans in a CPS. This shift in the role of humans, from being an operator of machines to a strategic decision-maker and a flexible problem solver, presents new design requirements for CPSs, particularly in terms of enhancing their ability to interact with humans [7]. Many technologies, such as an interactive human-machine interface [8], [9], a human digital twin [10] and a virtual-physical collaboration controller [11]

The associate editor coordinating the review of this manuscript and approving it for publication was Mark Kok Yew Ng .

have been designed for the interaction between CPSs and humans in the robotics domain. However, in comparison, despite the widespread study of the fault detection and diagnosis (FDD) problem in CPSs, most works focus solely on the development of FDD algorithms [12], [13], [14]. To date, limited works have proposed a comprehensive system-level CPS design that considers both physical components, simulation systems, and an interaction design specifically applied to FDD scenarios. Small errors in CPSs may lead to disastrous consequences. Even with the most recent advancements in FDD, human experts still (and in the foreseeable future continue to) play irreplaceable roles in anomaly response, particularly in safety-critical domains. To enable anomaly response technologies in CPSs to collaborate effectively and efficiently with humans, we must guarantee that the information provided by them to the humans about the anomaly (e.g., a system fault, an off-nominal behavior, or a cascading set of system disturbances) is not only accurate in and of

itself but also *epistemically accessible* or *explainable* to their human operators. In this paper, we will call anomaly response technologies with adequate epistemological underpinnings as *fault explanation (FE)*.

To give a more concrete example, it has great significance to monitor the process effectively and deal with abnormal conditions promptly to ensure the success of long-duration, deep space missions [15]. An Environmental Control and Life Support System (ECLSS), designed to meet the environmental and metabolic needs of the crew for such missions, is especially sensitive to failures since it directly relates to the crew's life and mission success [16]. Traditionally, the FDD method has been one of the core technologies to ensure the system's normal operation. However, humans, either onboard crew members or remote operators, have an irreplaceable advantage in the face of unpredictable anomalies. Thus, generating explanations for anomalies is indispensable in making anomaly response technologies more complete.

*Related Work:* Formal methods can serve as a starting point for developing FE technologies [17]. Existing formal verification tools can generate either a counterexample or a certificate to justify whether a CPS violates or satisfies a specification, which describes the desired/normal behavior [18]. Such certificates and counterexamples, particularly the latter, can already provide humans with some rudimentary understanding of the fault (which violates the specification) under investigation. However, the specification needs to be provided prior to the FE process, which may not be possible in many anomaly response scenarios. An alternative way is to learn the desired/normal or undesired/abnormal behavior of a CPS from data [19], [20], [21], [22]. For instance, a (temporal) logical formula can be learned from the time series data of normal (positive) and abnormal (negative) behaviors to classify these two different types of behaviors. However, formulas learned in such a data-driven fashion can only explain "What has happened?" not "Why has the fault happened?", a more practically important question in anomaly response. Moreover, it is difficult for such methods to generate explanations for token (singular) cases if they are unseen in the data, e.g., corner cases.

Causality theory [23], [24], [25] offers a wide range of tools to address these issues. It provides mathematical formulations to define and reason about cause-effect relationships, a crucial step towards answering "Why" questions. Moreover, based on studies on how humans explain decisions to one another [26], it has been shown that causal explanations are preferred by humans. Therefore FE systems should be able to provide causal explanations, if possible. There have been some recent efforts on integrating formal methods and causality, even though not in the context of FE. For instance, a new temporal logic was proposed in [24] to characterize cause-effect relationships and causal inference was then used to learn logical formulas from data. The method is data-driven therefore doesn't utilize knowledge of the system under investigation. Moreover, the proposed logic is associational, which doesn't take the full advantage of causality theory

(Pearl's causal hierarchy [23] consists of three layers from the least to most powerful: associational, interventional, and counterfactual). Ideally, a comprehensive explanation for a fault should include the description of the abnormal behavior, identification of the cause, and quantification of the causal relationship between the cause and the behavior [27]. However, existing fault explanation (FE) methods, such as requirement learning methods [19], [20], [21], [22] discussed above only capture the characteristics of the abnormal behavior, lacking causal implications. Despite the work in [24] attempts to express causal relationships by using temporal logic, the Probabilistic Causation [28] it chooses as the metric often fails to distinguish spurious correlations.

Considering the issues mentioned above, we propose a temporal logic as the formal explanation that can not only capture the properties of abnormal behavior and the corresponding potential causes but also provide a quantitative description to measure the causal effect of the potential cause for the abnormal behavior. Further, we propose an algorithm to infer this causal explanation, which serves as the crucial technology to solve the FE problem. The proposed explanation method sheds light on the way for the interaction design in CPSs, particularly under the human-involved FDD scenario.

*Contributions:* The main contribution of this paper is three-fold. First, we propose a new logic, Causal Signal Temporal Logic (CaSTL), which can be used to specify and reason about cause-effect relationships pertaining to FE. We endow CaSTL with interventional and counterfactual syntax and semantics. To the best of our knowledge, this is the first instance where a temporal logic has been proposed to incorporate the interventional and counterfactual aspects of causality. Second, we develop an algorithm that, given the simulation model of a system and the time series data of a fault, can infer a CaSTL formula explaining the fault from a causal perspective. Our algorithm is both model-based and data-driven. It generates an explanation that is consistent with both the observational data and the knowledge about the system. Finally, we validate the effectiveness of the proposed method via a simulated ECLSS developed by us.

## II. PRELIMINARIES

The formal definition of CPS is firstly proposed in [3] as: "CPS is an integration of computation with physical processes whose behavior is defined by both cyber and physical components of the system. Embedded computers and networks monitor and control the physical processes, with feedback loops where physical processes affect computations and vice versa." The cyber elements include embedded systems and network controllers, which are usually modeled as discrete events. Whereas the physical components exhibit continuous dynamics and are commonly modeled using differential equations [29]. For example, in our work, an ECLSS is considered a CPS composed of cyber components, e.g., some flight software supervision control and data acquisition systems, and physical components such as an array of

sensors and actuators that interact with the internal or external environment.

In the context of our FE problem, upon observing an abnormal behavior in a physical component, such as an actuator in an ECLSS, humans are naturally inclined to engage in causal reasoning [26]. Often, we believe (or want to believe) that one action caused another. It is a truth universally echoed by scientists that correlation does not imply causation. In daily life, however, the former is frequently mistaken for the latter. Causal inference aims at estimating the causal effects of an intervention or treatment on an outcome, which increasingly plays a vitally important role in scientific investigations and real-world applications [23], [24], [25]. Next, we will present a few key concepts in causality that are relevant to the rest of the paper. We use capital letters to denote variables, e.g.,  $X$ , and small letters to denote their values, e.g.,  $x$ . Similarly, we will use bold capital letters to denote sets of variables, e.g.,  $\mathbf{X}$ , and bold small letters to denote sets of values, e.g.,  $\mathbf{x}$ . If a set is indexed, e.g., with  $\mathbf{X}$  being a vector, we will use subscripts to denote its elements, e.g.,  $\mathbf{X}_i$  being  $\mathbf{X}$ 's  $i$ -th element/dimension (and similarly  $\mathbf{x}_i$  being the value of  $\mathbf{X}_i$ ).

In order to place generating an explanation for CPSs in the concept of causality, we first recall the original definition of the Structural Causal Model.

**Definition 1: Structural Causal Model (SCM)** [23]: An SCM is a triple  $M = \langle \mathbf{U}, \mathbf{V}, \mathbf{F} \rangle$ , where  $\mathbf{U}$  is a finite set of background or exogenous variables, which cannot be observed or experimented on,  $\mathbf{V}$  is a finite set of observable or endogenous variables (these variables are assumed to be functionally dependent on some subsets of  $\mathbf{U} \cup \mathbf{V}$ ), and  $\mathbf{F} = \{F_V | V \in \mathbf{V}\}$  is a finite set of functions such that each  $F_V$  is a mapping from a subset of  $\mathbf{U} \cup \mathbf{V} \setminus V$  to  $V$ .

A causal model  $M$  induces a directed (causal) graph,  $G(M)$ , where each vertex corresponds to a variable in  $\mathbf{U} \cup \mathbf{V}$  and each directed edge points from a variable in the domain of a function  $F_V$  (i.e.,  $Pa(V)$ ) to another variable in  $V$ . The (part of) physical component in a CPS can be transferred into an SCM where  $\mathbf{V}$  could represent a series of actuators' states at different time points, e.g.,  $X(t)$ ,  $\mathbf{F}$  represent any linear or non-linear functions to model dynamic relationships between the elements in  $\mathbf{V}$ . Generally speaking, in an SCM, the dynamics can be described using piece-wise functions [30] or differential equations [31]. In this paper, we assume the dynamics of actuators in our focused CPS are modeled by piece-wise functions and only consider the corresponding causal models that induce directed acyclic graphs (DAGs). Namely, for any element ( $X(t)$  for dynamic case) in  $\mathbf{V}$ , it has no effect on itself, i.e.,  $X(t)$  does not appear in  $F_{X(t)}$ . It has been shown in [25] that for an SCM that induces a DAG, the values of all its endogenous variables are determined given a context  $\mathbf{u}$ , i.e., a setting  $\mathbf{u}$  for all the exogenous variables in  $\mathbf{U}$ .<sup>1</sup> We call a pair  $(M, \mathbf{u})$  consisting of a causal model  $M$  and a context  $\mathbf{u}$  a (factual) causal setting (or a possible world).

<sup>1</sup>The reverse is not true though. There might be multiple  $\mathbf{u}$ 's corresponding to the same set of endogenous variable values.

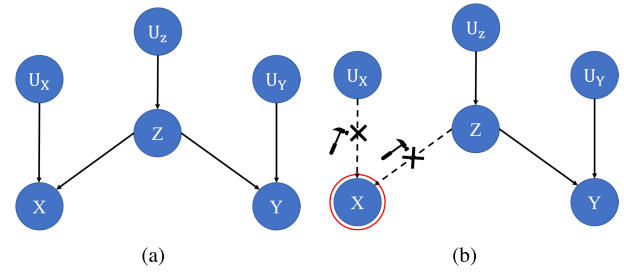


FIGURE 1. The causal graph  $G(M)$  induced by the SCM of Example 1.

To make it easier to understand, we give an example of a static SCM without introducing time  $t$ .

**Example 1:** Fig. 1. (a) shows the causal graph  $G(M)$  induced by an SCM  $M$ , where  $\mathbf{U} = \{U_X, U_Y, U_Z\}$ ,  $\mathbf{V} = \{X, Y, Z\}$ , and  $\mathbf{F} = \{F_X, F_Y, F_Z\}$ , e.g.,  $X = F_X(Z, U_X) = 5Z + 3U_X$ ,  $Y = F_Y(Z, U_Y) = 4Z + 7U_Y$ .

In the above example, we can observe  $X$  and  $Y$  are correlated since they're both caused by  $Z$ . However, there is no causal relationship between  $X$  and  $Y$ . Such structures widely exist in physical systems, e.g., two or more lights controlled by a single switch. However, we cannot determine the causal relationship between  $X$  and  $Y$  by only observing  $X$  and  $Y$ . Instead, we will need to conduct an intervention, which can be understood as a mathematical formulation of randomized experiments.

**Definition 2: Intervention** [23]: Forcing the value of some variable  $V \in \mathbf{V}$  to  $v$  in an SCM  $M$  (called an "intervention" and denoted by  $\text{do}(V = v)$ ) results in a new SCM denoted by  $M_{\text{do}(V=v)}$ . In the new SCM (called "intervention SCM" or "submodel"), the function for  $V$ ,  $F_V$ , is set to  $v$  while the remaining functions in  $\mathbf{F}$  are unchanged. A pair  $(M_{\text{do}(V=v)}, u)$  consisting of a submodel  $M_{\text{do}(V=v)}$  and a context  $u$  represents a counterfactual causal setting (or a parallel world). An intervention can be carried out on multiple endogenous variables simultaneously, denoted by  $\text{do}(\mathbf{X} = x)$ , where  $\mathbf{X} \subseteq \mathbf{V}$ . The resulting submodel is denoted by  $M_{\text{do}(\mathbf{X}=x)}$ .

**Example 2:** (Continued). An intervention  $X = x$  means that we should replace the original function  $F_X$  which maps from  $U_X$  and  $Z$  to  $X$  with a new function  $X = x$ . In Fig. 1. (b), this corresponds to removing the edges from  $U_X$  and  $Z$  to  $X$  and setting the value of node  $X$  to  $x$ .

It can be easily seen that if all functions in  $\mathbf{F}$  of an SCM  $M$  or a submodel  $M_{\text{do}(V=v)}$  are deterministic (an assumption we make in this paper), for a given context  $\mathbf{u}$ , there is only one possible value for each  $v \in V$ . We call the resulting set of endogenous variable values  $\mathbf{v}(M, \mathbf{u})$  or  $\mathbf{v}(M_{\text{do}(V=v)}, \mathbf{u})$  as *potential outcome*. With such, we can use any appropriate logic, e.g., the propositional or predicate logic, to reason about (factual and counterfactual) causal settings. For instance, given a formula  $\varphi := y > 5$ , a causal model  $M$  satisfies  $\varphi$  under context  $\mathbf{u}$ , written as  $(M, \mathbf{u}) \models \varphi$ , if  $y(M, \mathbf{u}) > 5$ . Moreover, Halpern and Pearl have proposed a definition of actual cause with the aforementioned formalism.

**Definition 3: HP Definition of Actual Cause** [25]:  $\mathbf{X} = x$ ,  $\mathbf{X} \subseteq \mathbf{V}$  is an actual cause of  $\varphi$  under the causal setting

$(M, \mathbf{u})$  if all the following conditions hold: (1) **Sufficiency**:  $(M, \mathbf{u}) \models \varphi$  and  $(M, \mathbf{u}) \models \mathbf{X} = \mathbf{x}$ ; (2) **Necessity**: There exists an intervention  $\text{do}(\mathbf{X} = \mathbf{x}')$  with  $\mathbf{x}' \neq \mathbf{x}$  such that  $(M_{\text{do}(\mathbf{X}=\mathbf{x}')} , \mathbf{u}) \not\models \varphi$ .

### III. CaSTL: CAUSAL SIGNAL TEMPORAL LOGIC

Even though the HP definition of actual cause can be used to reason about causality in many real life scenarios [25], it is not powerful enough for the purpose of explaining and reasoning about faults in CPSs, e.g., ECLSS, where temporal information is crucial for both the description of faults and the analysis of their causes. Thus, in this section, we extend **Dfn. (3)** and propose the syntax as well as the qualitative and quantitative semantics of Causal Signal Temporal Logic (CaSTL).

**Definition 4: Syntax of CaSTL:** The syntax of CaSTL is defined as follows:  $\Phi ::= \text{do}(\varphi_c) \rightsquigarrow \varphi_e$ , where  $\rightsquigarrow$  is the “lead-to” operator and  $\varphi_c$  and  $\varphi_e$  are the cause and effect event formulas, respectively, which have the same syntax as the Signal Temporal Logic (STL) [32]:  $\varphi_\varrho ::= X_\varrho(t_\varrho) \sim d_\varrho | \varphi_1 \wedge \varphi_2 | \varphi_1 \vee \varphi_2 | \diamond_{[\tau_1, \tau_2]} \varphi | \square_{[\tau_1, \tau_2]} \varphi$ , where subscript  $\varrho = \{c, e\}$ ,  $X_\varrho(t_\varrho)$  denotes the value of variable  $X_\varrho$  at time  $t_\varrho$ ,  $t_\varrho \in \mathbb{N}$ ,  $d_\varrho \in \mathbb{R}$ , and  $\sim \in \{\leq, <, >, \geq\}$ . The Boolean operators  $\vee$  and  $\wedge$  are disjunction (“or”) and conjunction (“and”), respectively. The temporal operators  $\diamond$  and  $\square$  stand for “eventually” and “always,” respectively. CaSTL is equipped with qualitative and quantitative semantics defined as follows.

**Definition 5: Qualitative Semantics of CaSTL:** A causal setting  $(M, \mathbf{u})$  (or the resulting trace  $\pi(M, \mathbf{u})$ ) satisfies  $\Phi$ , i.e.,  $(M, \mathbf{u}) \models \Phi$  (or  $\pi(M, \mathbf{u}) \models \Phi$ ) if and only if the following two conditions are satisfied: (1) **Sufficiency**:  $\forall \text{do}([X_c(\tau_1) = x_c(\tau_1), \dots, X_c(\tau_n) = x_c(\tau_n)])$  such that  $\pi_c = [x_c(\tau_1), \dots, x_c(\tau_n)] \models \varphi_c$ , i.e.,  $\pi_c \models \diamond_{[\tau_1, \tau_n]}(X_c \geq d_c)$ ,  $\pi(M_{\text{do}(\pi_c)}, \mathbf{u}) \models \varphi_e$ , i.e.,  $\pi(M_{\text{do}(\pi_c)}, \mathbf{u}) \models \square_{[\tau_3, \tau_4]}(X_e \geq d_e)$ . Here  $X_c$  is the variable related to the cause and  $X_e$  is related to the effect. (2) **Necessity**:  $\exists \text{do}([X_c(\tau_1) = x'_c(\tau_1), \dots, X_c(\tau_n) = x'_c(\tau_n)])$  such that  $\pi'_c = [x'_c(\tau_1), \dots, x'_c(\tau_n)] \not\models \varphi_c$ , i.e.,  $\pi'_c \not\models \diamond_{[\tau_1, \tau_n]}(X_c \geq d_c)$ ,  $\pi(M_{\text{do}(\pi'_c)}, \mathbf{u}) \not\models \varphi_e$ , i.e.,  $\pi(M_{\text{do}(\pi'_c)}, \mathbf{u}) \not\models \square_{[\tau_3, \tau_4]}(X_e \geq d_e)$ .

**Remark 1:** Intuitively, according to our semantics, we say that  $\varphi_c$  is the cause of  $\varphi_e$  in the context of an SCM  $M$  (e.g., one converted from a simulation model) and a context  $u$  iff (1) any intervention satisfying  $\varphi_c$  will always result in a trace satisfying  $\varphi_e$  and (2) there exists an intervention violating  $\varphi_c$  which will result in a trace violating  $\varphi_e$ . We are extending the HP definition of token cause (**Dfn. (3)**) here, i.e., “if the cause  $\varphi_c$  had not occurred, then the effect  $\varphi_e$  would not have happened” (also called the counterfactual principle). Different from the original HP definition, which doesn't naturally afford reasoning about temporal relationships, our CaSTL definition of token cause (by combining the powers of causality and temporal logic) enables us to reason about and explain both causal and temporal relationships. Moreover,  $\varphi_c$  of CaSTL is more expressive than the HP causal expression, either a single variable or a set of variables.

The qualitative semantics can be used to check whether a causal setting  $(M, u)$  satisfies or violates a proposed causal relation expressed in CaSTL. However, it does not provide any information about how strongly the **Sufficiency** and **Necessity** are satisfied or violated. Quantitative semantics for STLs, called robustness degrees, has been proposed to provide a measure of satisfiability of a trace with respect to (w.r.t.) a STL formula [33], [34]. We define the qualitative semantics of CaSTL by modifying these existing definitions as follows:

**Definition 6: Quantitative Semantics of CaSTL:** The degrees of sufficiency and necessity of a causal setting  $(M, u)$  (or the resulting trace  $\pi(M, \mathbf{u})$ ) w.r.t.  $\Phi$  are defined as:

(1) The **degree of sufficiency** of a CaSTL formula  $\Phi$  w.r.t. a model  $M$  and a trace  $\pi$  is

$$S(\Phi) = \mathbb{E}[\rho_e(\varphi_e, \pi(M_{\text{do}(\pi_c)}, \mathbf{u})) | \forall \rho_c(\varphi_c, \pi_c) > 0], \quad (1)$$

where  $\rho_c(\cdot)$  are the robustness degrees of the interventional traces  $\pi_c$  w.r.t. the cause formula  $\varphi_c$  (see **Dfn. 5**), which is calculated based on [34].  $\rho_e(\cdot)$  are the robustness degrees of the traces  $\pi(M_{\text{do}(\pi_c)}, \mathbf{u})$  w.r.t. the effect formula  $\varphi_e$ . Both of these two robustness degrees are bounded to the interval  $[-1, 1]$ . Therefore,  $\rho_c(\cdot) > 0$  are corresponding to traces generated by applying interventions satisfying  $\varphi_c$ .

(2) The **degree of necessity** of a CaSTL formula  $\Phi$  w.r.t. a model  $M$  and a trace  $\pi$  is defined as

$$N(\Phi) = -\mathbb{E}[\rho_e(\varphi_e, \pi(M_{\text{do}(\pi'_c)}, \mathbf{u})) | \forall \rho'_c(\varphi_c, \pi'_c) < 0], \quad (2)$$

where  $\rho'_c(\cdot)$  are the robustness degrees of the interventional traces  $\pi'_c$  that violate the cause formula  $\varphi_c$  (see **Dfn. 5**).  $\rho_e(\cdot)$  are the robustness degrees of the traces  $\pi(M_{\text{do}(\pi_c)}, \mathbf{u})$  w.r.t. the effect formula  $\varphi_e$ . Similarly,  $\rho'_c(\cdot) < 0$  are corresponding to traces generated by applying interventions violating  $\varphi_c$ .

### IV. PROBLEM FORMULATION: FAULT EXPLANATION FROM A CAUSAL PERSPECTIVE

Based on the fact that causal inference is not possible without manipulating the variable(s) to which a cause will be attributed to, we will utilize a simulation model  $M$  of the system of interest, such as an ECLSS, to provide causal explanations for anomalies.

**Problem 1: Fault Explanation (FE) Problem.** Given a fully observable simulation model  $M$  of the system of interest, e.g., an ECLSS, the time series data (trace) of a fault  $\pi = [\mathbf{x}(0), \dots, \mathbf{x}(T)]$ , the time series data (trace) of a normal behavior  $\pi^* = [\mathbf{x}^*(0), \dots, \mathbf{x}^*(T)]$ , and a formula  $\varphi_e$  describing the effect of the fault, find another formula  $\varphi_c$  (i.e., find the variable  $X_c$ , the time bond  $[t_{c1}, t_{c2}]$ , and the threshold  $d_c$ ) such that the CaSTL formula  $\Phi = \text{do}(\varphi_c) \rightsquigarrow \varphi_e$  explains fault  $\varphi_e$  in the context of model  $M$  and trace  $\pi$  in the sense that: (1) **Existence**: there should be at least one context  $\mathbf{u}$  such that  $\pi = \pi(M, \mathbf{u})$ , i.e., the trace generated by  $M$  and  $u$  satisfies  $\pi \models \varphi_c$  and  $\pi \models \varphi_e$ . Moreover,  $\pi^* \not\models \varphi_c$  and  $\pi^* \not\models \varphi_e$ . (2) **Sufficiency and Necessity**: For all contexts  $\mathbf{u}$ 's satisfying the **Existence** condition,  $(M, \mathbf{u}) \models \Phi$  according to the token level semantics of CaSTL, i.e., **Dfn. (5)**.



**Remark 2:** The assumption that  $\varphi_e$  is given is not a very strong one, given all the existing temporal logic inference algorithms [19], [20], [21], [22] that can be used to infer  $\varphi_e$  from data. We merely make the assumption to keep the paper compact. Besides, in practice,  $\varphi_e$  can be set according to the alarm threshold of the abnormal behavior.

**Remark 3:** We believe explanations written as CaSTL formulas are epistemically accessible to human operators. Such explanations satisfy a range of criteria of what humans see as “good” explanations [26]. For instance, CaSTL explanations are contrastive. Humans tend to think in counterfactual cases, e.g., “What would have happened if variable  $X$  had been different?” CaSTL naturally affords this aspect in its semantics. Furthermore, CaSTL explanations are compact due to the expressiveness of CaSTL as mentioned in **Remark 1**. At last but not least, CaSTL explanations can be selected. Human usually do not expect explanations that cover the complete list of causes of an event. We are used to selecting one or two causes from a list of possible causes as “the” explanation. As such, in our framework, we first compute the degrees of sufficiency and necessity of each possible cause and then only provide those with the highest degrees to humans.

## V. METHODOLOGY

In this section, we will first convert the FE problem into an optimization problem (**Sec. V. V-A**). Then we introduce a way of formulating simulation models as SCMs (**Sec. V. V-B**) and propose a method to generate traces for quantifying the degrees of sufficiency and necessity (**Sec. V. V-C**). Finally, we present an overall algorithm to solve the FE problem (**Sec. V. V-D**).

### A. FE AS AN OPTIMIZATION PROBLEM

In practice, it is quite possible that there doesn't exist an explanation  $\Phi$  that satisfies all three conditions mentioned in **Problem 1**. To accommodate this, we will utilize the quantitative semantics of **Sufficiency** and **Necessity** defined in **Sec. III** and convert the FE problem to an optimization one. To identify the (possible) cause event  $\varphi_{c,i}$  associated with an element/dimension  $\mathbf{X}_i$  of a component  $\mathbf{X}$  (with the corresponding explanation being  $\Phi_i := \text{do}(\varphi_{c,i}) \rightsquigarrow \varphi_e$ ), we solve the following optimization problem:

**Problem 2: FE Optimization Problem.** Given a fully observable simulation model  $M$  of the system of interest, e.g., an ECLSS, the trace of a fault  $\pi = [x(0), \dots, x(T)]$  the trace of a normal behavior  $\pi^* = [x^*(0), \dots, x^*(T)]$ , a formula  $\varphi_e$  describing the effect of the fault, the dimension of interest  $\mathbf{X}_i$ , find the optimal value of parameter vector  $\theta_i^* := [t_{c1}^*, t_{c2}^*, d_c^*, \sim^*]$  (with the resulting CaSTL formula being  $\Phi_i^* = \text{do}(\varphi_{c,i}^*) \rightsquigarrow \varphi_e$ ) that solves the following optimization problem:

$$\sup J_i(\theta_i) = -E(\Phi_i) + \lambda_S S(\Phi_i) + \lambda_N N(\Phi_i) \quad (3)$$

where  $E(\Phi_i) = e^{-(\rho_{c\pi} - \rho_{c\pi^*})}$  is the degree of existence,  $\rho_{c\pi}$  and  $\rho_{c\pi^*}$  are robustness degrees of  $\pi$  and  $\pi^*$  w.r.t.  $\varphi_{c,i}$ , respectively.  $S(\Phi_i)$  and  $N(\Phi_i)$  are **degrees of sufficiency** and

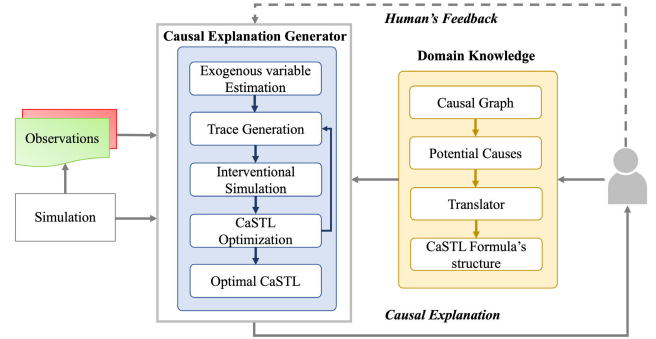


**FIGURE 2.** The framework of our proposed method. The dashed line is one of our future work. The proposed framework can not only provide causal explanations to human operators but also can be used to transmit human's feedback back Causal Explanation Generator to achieve a cooperative anomaly response.

**necessity** of the CaSTL formula  $\Phi_i$  (as defined in **Eqns. 1** and **2**),  $\lambda_S$  and  $\lambda_N$  (both positive) balance the degrees of existence, sufficiency and necessity.

Finally, with all the  $\Phi_i^*$ 's ( $\theta_i^*$ 's) and their corresponding costs  $J_i^*$ , we can select the ones with the lowest costs (highest combined degrees of existence, sufficiency, and necessity) and provide them to human operators.

### B. SIMULATION MODELS AS SCMS

From **Example 1**, we are informed that the framework of the causal inference needs to manipulate the variable(s) to which a cause will be attributed. Such interventions are clearly unfeasible in many real-life's cases; however, we can manipulate variables with the help of simulation models to take the intervention. Because in simulation models, it is often possible to manipulate a variable individually, this naturally conforms to the concept of intervention and thus facilitates causal inference.

In order to take advantage of the flexibility of the simulation model to solve the FE optimization problem from the perspective of the causal inference, such a model can be converted to an SCM as follows. First, set  $\mathbf{U}$  as the sensor noises. Second, set  $\mathbf{V}$  as the collection of all components of the state variable at all time instants, i.e.,  $\mathbf{V} = \{\mathbf{X}(0), \dots, \mathbf{X}(T)\}$ . Finally, set  $\mathbf{F}$  as  $\{F_{X(t)} | t = 0, \dots, T\}$  with each  $F_{X(t)}$  is the underlying relations among components.

### C. DEGREES OF SUFFICIENCY AND NECESSITY COMPUTATION

Based on **Def. 6**, we need to generate traces satisfying the cause formula  $\varphi_{c,i}$  to calculate the **degree of sufficiency**. As for the **degree of necessity**, traces violating  $\varphi_{c,i}$  need to be generated. We construct an optimization problem for trace generation. For preparing the calculation of the **degree of sufficiency**, we first solve the following problem:

$$\inf \left( -\sum_{n=1}^I \rho_{c_n} - \frac{1}{2} \sum_{n=1}^I \sum_{m=1}^I \|\rho_{c_n} - \rho_{c_m}\|^2 \right),$$

**Algorithm 1** Degrees of **sufficiency** and **necessity** Computation for  $\varphi_{c,i}$

**Input:** SCM  $M$  (converted from a simulation model), a causal STL formula  $\varphi_{c,i}$  with parameter set  $\theta_i$ , learning rates  $\gamma_1$  and  $\gamma_2$ , number of traces  $I$ , two thresholds  $\epsilon_{d_1}$  and  $\epsilon_{d_2}$

**Output:** The **degree of sufficiency**  $S(\Phi_i)$  and the **degree of necessity**  $N(\Phi_i)$

- 1: Obtain  $\mathbf{u}$  from the simulation model
- 2: **while**  $\min \|\rho_{c_n} - \rho_{c_m}\| \leq \epsilon_{d_1}$  **do**
- 3:   Solve **Eqn. (4)** using the gradient-descent method with  $\gamma_1$  as the learning rate
- 4: **end while**
- 5: Generate interventions using **Eqn. (6)**
- 6:  $S(\Phi_i) \leftarrow$  **Eqn. (1)**
- 7: **while**  $\min \|\rho'_{c_n} - \rho'_{c_m}\| \leq \epsilon_{d_2}$  **do**
- 8:   Solve **Eqn. (5)** using the gradient-descent method with  $\gamma_2$  as the learning rate
- 9: **end while**
- 10: Generate interventions using **Eqn. (6)**
- 11:  $N(\Phi_i) \leftarrow$  **Eqn. (2)**
- 12: **return**  $S(\Phi_i)$  and  $N(\Phi_i)$

$$\begin{aligned} \text{s.t.} \quad & \pi_{c,i} \models \varphi_{c,i}, \\ & \delta\rho_{c_i} \geq \delta\epsilon_{\min}, \end{aligned} \quad (4)$$

where  $I$  is the number of traces to be generated,  $\rho_{c_i}$  is the robustness degree of each trace in  $\pi_{c,i}$  w.r.t.  $\varphi_{c,i}$ , and the scalar  $\epsilon_{\min} \geq 0$  is a desired minimum robustness. According to the cost function in Eqn. (4),  $\forall \rho_{c_i} \in (0, 1]$ , the generated traces satisfy  $\varphi_{c,i}$  and the corresponding robustness degrees have a uniform distribution in the interval  $(0, 1]$ .

Similarly, for calculating the **degree of necessity**, we solve the following problem at first:

$$\begin{aligned} \inf & \left( \sum_{i=1}^I \rho'_{c_n} - \frac{1}{2} \sum_{n=1}^I \sum_{m=1}^I \|\rho'_{c_n} - \rho'_{c_m}\|^2 \right), \\ \text{s.t.} \quad & \pi'_{c,i} \not\models \varphi_{c,i}, \\ & \delta\rho'_{c_i} \leq -\delta\epsilon_{\min}, \end{aligned} \quad (5)$$

where  $\rho'_{c_i}$  is the robustness degree of each trace in  $\pi_{c,i}$  w.r.t.  $\varphi_{c,i}$ , which satisfy  $\forall \rho'_{c_i} \in [-1, 0)$ . Considering the smoothness of AGM robustness degree, we take a similar gradient-descent method proposed in [35] to solve the above problems. After that, we take interventions on the simulation model  $M$  using  $\pi_{c,i}$  and  $\pi'_{c,i}$ :

$$\pi(M_{\text{do}(\cdot)}, \mathbf{u}) = \pi(M_{\text{do}(X_c=\cdot)}, \mathbf{u}), \quad (6)$$

where  $\cdot$  is  $\pi_{c,i}$  and  $\pi'_{c,i}$ , respectively, and  $\mathbf{u}$  is the specific sensor noises. Finally, the degrees of **sufficiency** and **necessity** can be computed using **Eqs. (1)** and **(2)**. The algorithm to calculate the degrees of **sufficiency** and **necessity** is shown in **Alg. 1**.

#### D. SOLUTION

The conventional approaches for the optimization of cost functions  $J_i$  are often expensive, because the number of

evaluations that may be performed is limited, typically to a few hundred or even less [36]. In our problem, we evaluate  $J_i$  using a simulator, e.g., a Simulink model. Given the complexity of many CPS models, obtaining a trace from the simulator can be time-inefficient and it is hard to observe the first- or second-order derivatives when evaluating  $J_i$ . Therefore, to learn a CaSTL formula in an efficient manner, we need to decrease the number of simulations and choose a more time-efficient optimization approach such as the Bayesian optimization (BayesOpt). Combined with our focus on finding a global rather than local optimum, we decide to use BayesOpt since it provides an elegant framework for avoiding getting caught in a local minimum.

BayesOpt consists of two main components: a Bayesian statistical model, typically Gaussian process (GP) regression, for modeling the cost function, and an acquisition function for deciding where to sample next. Let  $J(\cdot) \sim GP(m(\theta), k(\theta, \theta'))$  in Eqn. (3) be an unknown function we aim to optimize over a candidate set  $\theta = [t_{c_1}, t_{c_2}, d_c]$ . This GP is completely specified by its mean function  $m(\theta)$  and its covariance function or kernel  $k(\theta, \theta')$ :

$$m(\theta) = \mathbb{E}[J(\theta)], \quad (7)$$

$$k(\theta, \theta') = \mathbb{E}[(J(\theta) - m(\theta))(J(\theta') - m(\theta'))]. \quad (8)$$

In this paper, the squared exponential kernel [37] is used in GP modelling, which can be computed as:

$$k(\theta_1, \theta_2) = \exp\left(-\frac{|\theta_1 - \theta_2|^2}{(2l)^2}\right), \quad (9)$$

where  $l$  is the length scale and  $|\cdot|$  is the Euclidean length.

The statistical model as shown in Eqn. (7) is then used to create an acquisition function  $\alpha_t(\theta)$ . As such, it can be used to suggest  $P_t$ , the next input with which to sample the system. Gaussian Process Upper Confidence Bound (GP-UCB) [38] is one intuitive acquisition function. It balances exploration and exploitation through a single hyperparameter,  $\beta_t$ :

$$\alpha_t(\theta) = m_{t-1}(\theta) + \sqrt{\beta_t} \sigma_{t-1}(\theta), \quad (10)$$

A higher  $\beta_t$  increases the variance of the acquisition function favor points, causing more exploration. A lower  $\beta_t$  increases the mean of the acquisition function favor points, causing more exploitation.

The algorithm to solve **Problem 2** using the BayesOpt is shown in **Alg. 2**. The steps are self-explanatory. We adopt the classical approach of counterfactual reasoning: abduction (Line 1) and intervention, consisting of action and prediction (Lines 7-9). The code will be available here. **Fig. 2** shows the framework of our proposed methods to solve the **FE** problem.

## VI. CASE STUDY

### A. ECLSS SIMULATION MODEL

The Simulation Testbed for Exploration Vehicle ECLSS (STEVE) at the University of Colorado Boulder is a simplified single-bed  $CO_2$  removal system of the Carbon Dioxide Removal Assembly (CDRA) onboard the International Space

**Algorithm 2** FE Optimization for  $\varphi_c(\theta)$ 

**Input:** Search space  $D$ , SCM  $M$  (converted from a simulation model), fault trace  $\pi$ , normal trace  $\pi^*$ , effect event  $\varphi_e$

**Output:** A CaSTL formula that explains fault trace  $\pi$  in the context of model  $M$ :  $\Phi_i^* = \text{do}(X_i(t_c^*) \sim^* d_c^*) \rightsquigarrow \varphi_e$  and its cost  $J_i^*$

- 1: Obtain  $\mathbf{u}$  from the simulation model
- 2: Select  $\theta \in D$  for every different  $\varphi_c$
- 3: Calculate  $J$  using **Eqn. (3)** and  $M$
- 4:  $P_0 \leftarrow [\theta, J]$
- 5: **for**  $t$  in  $[1, T]$  **do**
- 6: Bayesian update  $m_{t-1}(\theta)$  and  $\sigma_{t-1}(\theta)$
- 7:  $\theta_t \leftarrow \text{argmax}_{\theta \in D} m_{t-1}(\theta) + \sqrt{\beta_t} \sigma_{t-1}(\theta)$
- 8: Calculate  $S$  and  $N$  using **Alg. 1**
- 9: Calculate  $J_t$  using **Eqn. (3)**
- 10:  $P_t \leftarrow P_{t-1} \cup (\theta_t, J_t)$
- 11: **end for**

Station (ISS). Its purpose is to simulate common anomalies of CDRA and generate data under nominal and/or faulty conditions. STEVE, shown in **Fig. 3**, comprises a single sorbent bed packed with a 13X zeolite used in the 4-Bed  $\text{CO}_2$ , a successor of the Carbon Dioxide Removal Assembly (CDRA). As indicated in the Piping and Instrumentation Diagram (**Fig. 4**), the bed either removes  $\text{CO}_2$  from the provided air flow (adsorption) or releases  $\text{CO}_2$  under thermal vacuum (desorption). During adsorption, the apparatus supplies the specified flow of  $\text{CO}_2$ -laden air to the sorbent bed. Nominally, STEVE provides a gas mixture with 78.86% nitrogen, 20.84% oxygen, 0.3% carbon dioxide, and dew point of less than  $-60^\circ \text{C}$ ; the latter achieved with a desiccant bed packed with Drierite® beads. At this concentration, the  $\text{CO}_2$  partial pressure is approximately 2.1 mm Hg. A rope heater raises the insulated bed temperature to  $200^\circ \text{C}$  and a throttled vacuum pump reduces pressure to below 20 mm Hg for  $\text{CO}_2$  desorption and regeneration of the pellets via thermal-pressure swing. The adsorption/desorption cycle can be repeated for a set number of cycles.

In parallel, a Simulink model of the STEVE testbed was developed. The model can rapidly generate data and simulate conditions that the STEVE testbed cannot experimentally test. The model also utilizes Simscape, a physical pre-developed component model used in the Simulink environment. **Fig. 5** shows the overall model that comprises principal components and subsystems of the STEVE testbed, which are the inlet stream, the sorbent bed, valves, sensor suites, vacuum pump, flow controller, filter, and pipes.

The Simscape Moist Air components assume that gas species in the mixture are thermally perfect. Relationships between pressure, temperature, and density obey the ideal gas law. Other properties – specific enthalpy, specific heat, dynamic viscosity, and thermal conductivity – are functions of temperature only. The Simscape models conserve mass, momentum, and energy based on this assumption. In addition,

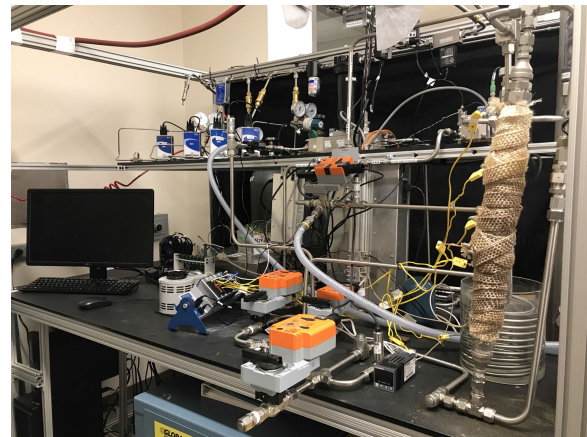


**FIGURE 3.** Image of the STEVE testbed.

Gaussian noise is added to the simulation results at the Data Acquisition (DAQ) subsystem to simulate sensor noise and saturation. Although these Simscape components enable fast and effortless simulation of basic thermal and fluid properties, there are no pre-developed models for valves and the sorbent bed which performs  $\text{CO}_2$  adsorption and desorption. Such models are hard-coded using the “MATLAB Function block” available in the Simulink library.

The Simulink model is designed to simulate multiple failure modes similar to the STEVE testbed. For example, a leak at the outlet of the sorbent bed, which may be caused by wear and tear of connectors or the human error during maintenance, can be simulated. Air will leak out of the system during adsorption and into the system during desorption due to the pressure difference between the bed and the lab (habitat) environment. For this study, we performed a simulation with four cycles that contain 80 minutes  $\text{CO}_2$  adsorption and 80 minutes desorption per cycle. (**Fig. 6 (b)** and **(c)**).

## B. SIMULATION RESULTS AND DISCUSSION

In order to validate the performance of proposed method for the FE problem, we consider the following situations: (1) there is a single fault happened to the component that we select as a potential cause and (2) there are multiple faults happened to different components that we select as potential causes.

### 1) SINGLE FAULT

In this case, a Leak failure is introduced to “Valve 1” in the third cycle as shown in **Fig. 6 (a)**. The corresponding anomalies can be observed in a sequences sensors, e.g. *Bed Temperature*,  *$\text{CO}_2$  Concentration*, etc., as shown in **Fig. 6 (b)**, **(c)**. In this case study, we made some simplifications and only analyzed the causal relationship between two components. Next, we follow our proposed framework as shown in **Fig. 2** to infer a CaSTL to explain this fault qualitatively and quantitatively:

1. The developers of this ECLSS provide a causal graph of this failure mode, as shown in **Fig. 7**.

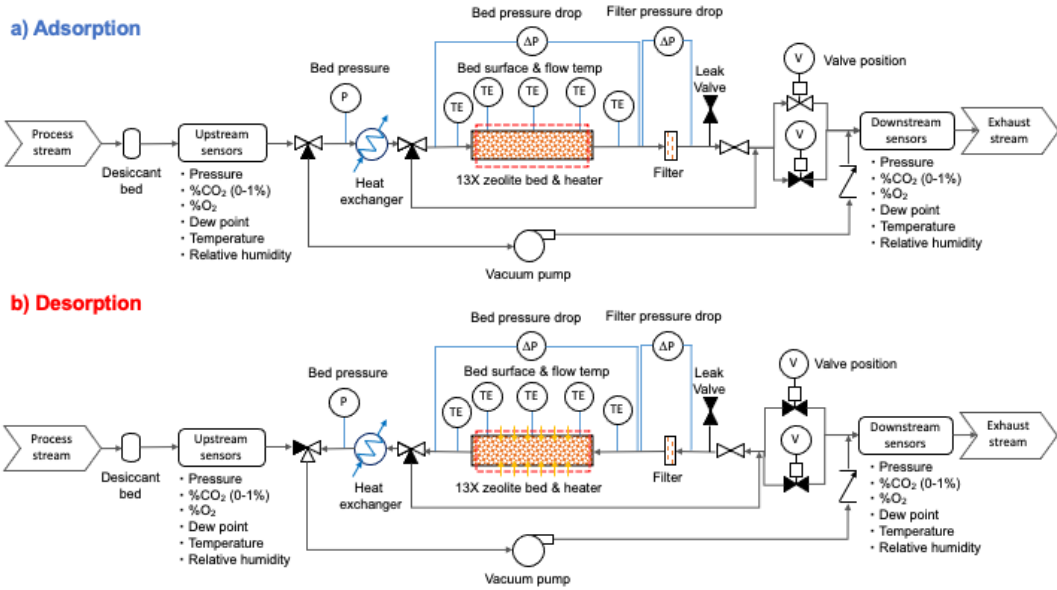


FIGURE 4. STEVE Piping and Instrumentation Diagram.

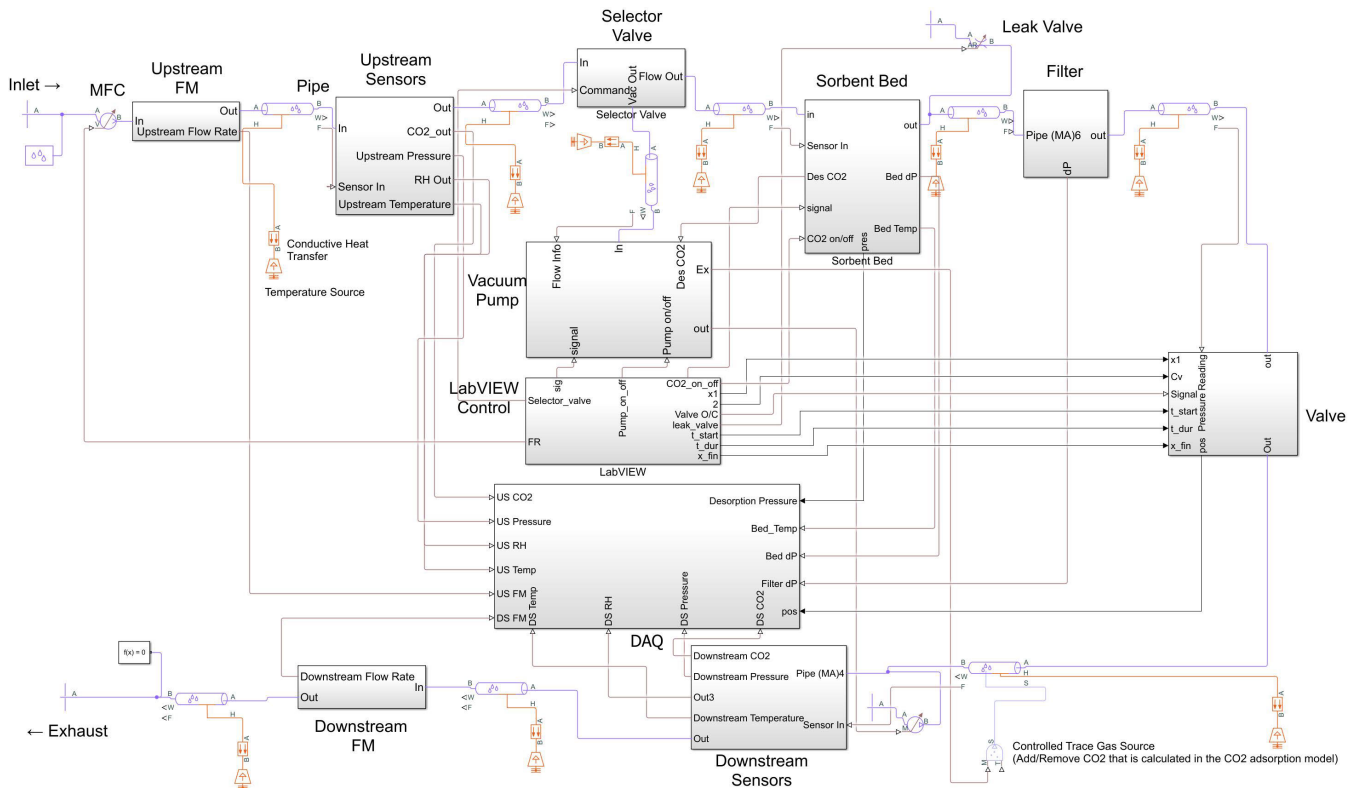


FIGURE 5. Overview of the Simulink Model.

- Determine the abnormal behavior, the value of sensor *CO<sub>2</sub> Concentration* is below the threshold 87% (the purple dash line as shown in Fig. 6.(c)) at time bonds [424 min, 431 min], as the effect for our problem.

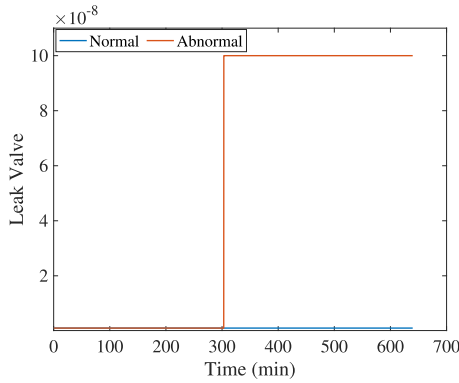
This can be written in the effect STL as  $\varphi_e := \square_{[424,431]}(CO_2 \leq 87\%)$ .

- Determine the potential cause of this particular abnormal behavior could be a leak of “Valve 1”. This cause can

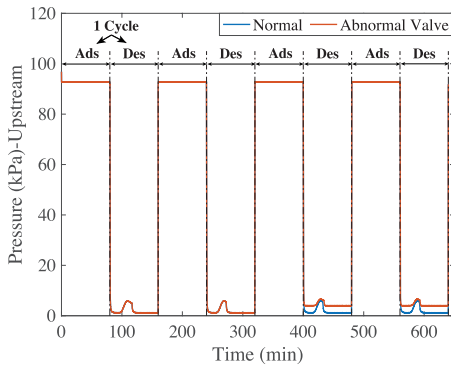


TABLE 1. FE Results for Case 1.

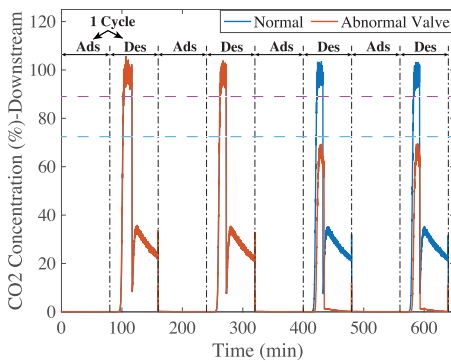
Effect Formula	CaSTL Explanation $\Phi_i^*$	$S(\Phi^*)$	$N(\Phi^*)$
$\varphi_e := \square_{[424,431]}(CO_2 \leq 87\%)$	$do(\square_{[310,428]}(Leak \geq 7.2 \times 10^{-8} \wedge Leak \leq 2.3 \times 10^{-7})) \rightsquigarrow \varphi_e$	0.54	0.68
$\varphi_e := \square_{[424,431]}(CO_2 \leq 71\%)$	$do(\square_{[308,425]}(Leak \geq 9.2 \times 10^{-8} \wedge Leak \leq 2.2 \times 10^{-7})) \rightsquigarrow \varphi_e$	0.63	0.72



(a)



(b)



(c)

FIGURE 6. In (a)-(c), the blue (red) trajectory corresponds to a normal (abnormal) behavior of the system used in the case study. Please notice that in paper, we assume we have access to the abnormal behaviors as the fault trace  $\pi$  and the normal ones as  $\pi^*$ . Each cycle includes one  $CO_2$  adsorption (ads) cycle and one desorption (des) cycle. (a) illustrates the “real” cause, an abrupt fault artificially injected; while the purple and blue dash lines in (c) illustrate two thresholds to define different effect formulas  $\varphi_e$ , respectively.

be written in a cause STL as  $\varphi_c := \square_{[t_1, t_2]}(Leak \geq \alpha \wedge Leak \leq \beta)$ .

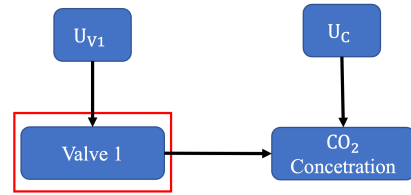


FIGURE 7. The causal graph pertaining to case 1, there is a leak happened to Valve 1. And this failure mode (red box) has an effect on  $CO_2$  concentration.

- Given the abnormal and normal behaviors shown in Fig. 6. (a) and (c), we infer the optimal parameters in the CaSTL,  $\Phi := do(\square_{[t_1, t_2]}(Leak \geq \alpha \wedge Leak \leq \beta)) \rightsquigarrow \square_{[424,431]}(CO_2 \leq 87\%)$ , following steps listed in the blue box in Fig. 2 using Alg. 2.

Table 1 shows the formulas learned using our algorithm. It can be observed that  $\Phi_1^* := do(\square_{[310,628]}(Leak \geq 8.2 \times 10^{-8} \wedge Leak \leq 2.3 \times 10^{-7})) \rightsquigarrow \varphi_e$  not only precisely locates the time bond  $t \in [310 \text{ min}, 628 \text{ min}]$  but also approximately locates the leakage range of the valve,  $Leak \in [8.2 \times 10^{-8}, 2.3 \times 10^{-7}]$ . Compare this with the real cause shown in Fig. 6. (a), we can observe that the learned formula correctly the temporal and spatial properties of the injected fault. Next, we change the threshold from 81% to 71% (the blue dash line as shown in Fig. 6.(c)) in the effect formula  $\varphi_e := \square_{[424,431]}(CO_2 \leq 71\%)$  and then infer the parameters in the cause formula,  $\varphi_c := \square_{[t_1, t_2]}(Leak \geq \alpha \wedge Leak \leq \beta)$ . The corresponding results are shown in Table 1. According to the results, we can observe that for different effects, even for cause formulas have the same form, the parameters inferred in the cause formulas are different, and the corresponding **Sufficiency** and **Necessity** are also different. This is because the cause formula on the one hand should capture the difference between abnormal and normal behavior (as shown in Fig. 6), and provide the best explanation for different outcomes on the other hand, that is maximizing  $N$  and  $S$ .

## 2) MULTIPLE FAULTS

In this case, we inject a fault mode, a leak, into Valve 1 and another fault, valve stiction, into Valve 2, which is the “Valve” model in Fig. 5. These two valves nominally open and close during adsorption and desorption, respectively. The corresponding causal graph is shown in Fig. 8. The corresponding anomalies can be observed in a sequences sensors as shown in Fig. 9. (a)-(c). We define the abnormal behavior as  $\varphi_e := \square_{[424,431]}(CO_2 \leq 71\%)$  for this case. And we set the causes are related to (1) the leak of Valve 1, written as  $\varphi_{c1} := \square_{[t_1, t_2]}(Leak \geq \alpha \wedge Leak \leq \beta)$ ; and (2) the

TABLE 2. FE Results for Case 2.

Effect Formula	CaSTL Explanation $\Phi_i^*$	$S(\Phi^*)$	$N(\Phi^*)$
$\varphi_e := \square_{[424,431]}(CO_2 \leq 71\%)$	$do(\square_{[307,423]}(Leak \geq 9.4 \times 10^{-8} \wedge Leak \leq 2.4 \times 10^{-7})) \rightsquigarrow \varphi_e$	0.66	0.72
$\varphi_e := \square_{[424,431]}(CO_2 \leq 71\%)$	$do(\square_{[215.3,417.7]}(Degree \leq 17.2)) \rightsquigarrow \varphi_e$	0.02	0.03

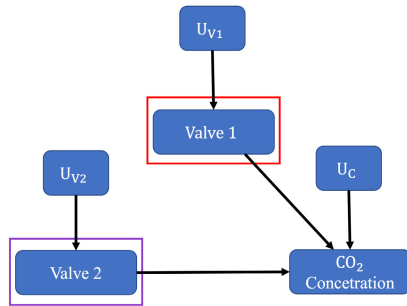
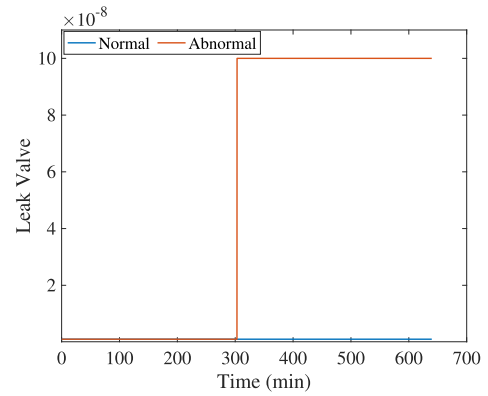


FIGURE 8. The causal graph pertaining to case 2, there is a leak (red box) happened to Valve 1. And there is another stiction (purple box) happened to Valve 2. Both of these two faults have effects on CO<sub>2</sub> concentration.

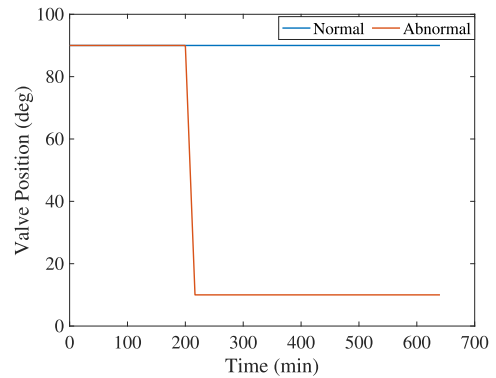
stiction of Valve 2, written as  $\varphi_{c2} := \square_{[t3,t4]}(Degree \leq \gamma)$ . Table 2 shows the learned formulas and the corresponding **Sufficiency** and **Necessity**. We can observe that both the **Sufficiency** and **Necessity** of cause related to Valve 2 are smaller than those related to Valve 1. This means Valve 1 has a stronger causal effect than Valve 2 for this specific abnormal behavior. From this, we are informed that different causes have different degrees of influence for the same effect.

To further validate the advantages of our proposed method, we compare it with two fault diagnosis (explanation) methods. For the data-driven fault diagnosis method, we choose the approach proposed in [39], which is able to extract and classify temporal properties of different fault modes based on the k-means classification method. For the other method, we choose an STL inferring approach proposed in [22], which is designed for learning an STL to capture the temporal properties of a fault mode. This method can be used as a post-hoc explanation to a classification approach, e.g., here we use it to explain the classification results generated by the data-driven fault diagnosis method [39]. In the comparison, we construct a dataset which includes the value of the valve, the position of the valve and CO<sub>2</sub> concentration corresponding the fault mode 1: a leak failure, fault mode 2: a stiction of a valve and the normal state. For fault mode 1, we generate 50 traces by randomly injecting a leak greater  $8 \times 10^{-8}$  after 300 min. For fault mode 2, we generate 50 traces by randomly injecting a leak greater  $8 \times 10^{-7}$  after 200 min and commanding valve position to partially open to 5° after 200 min. Finally, we generate 50 traces for the normal condition. We randomly select 80% of the traces for training a cluster [39] to differentiate these three modes and then learning correspond STLs [22] to describe properties of each fault modes while the remaining signals are used for testing. The results are shown in Table 3

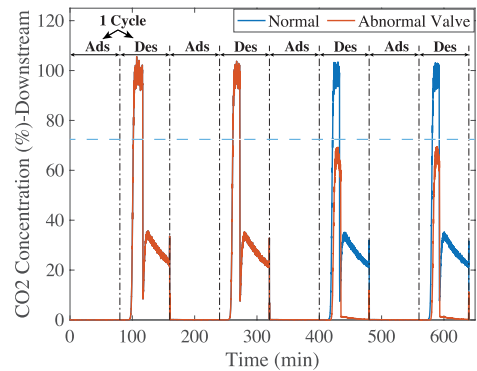
Here we would love to discuss the main difference between our work from other existing methods. Firstly, multiple tem-



(a)



(b)



(c)

FIGURE 9. The blue (red) trajectory corresponds to a normal (abnormal) behavior of the system used in the second case study. (a) illustrates a leak injected into Valve 1 and (b) illustrates a stiction injected into Valve 2. The blue dash lines in (c) illustrate the threshold to define effect formulas  $\varphi_e$  which describes the abnormal behavior related to CO<sub>2</sub> Concentration.

poral logic inference algorithms [19], [20], [21], [22] focus on inferring STLs that can capture the proprieties to differentiate

TABLE 3. Results of two data-driven methods.

Fault Mode	Accuracy		Learned Formula
	Method 1 [39]	Method 2 [22]	
Leak Valve (Valve 1)	100%	100%	$\square_{[308,535]}(Leak \geq 8.13 \times 10^{-8}) \wedge \square_{[600,640]}(CO_2 \leq 52\%)$
Stiction Valve (Valve 2)	100%	100%	$\square_{[212,576]}(Leak \geq 8.13 \times 10^{-8}) \wedge \square_{[270.4,501]}(Degree \leq 70.4) \wedge \square_{[452,489]}(CO_2 \leq 55\%)$

the abnormal behaviors from the normal ones. These STLs are somehow interpretable for human users; however, the learned properties, e.g., the learned formulas in Table 3, do not have any causal implications. Similarly, many components in an ECLSS statistically correlate with each other. Therefore, it is quite possible that a purely data-driven method may wrongly identify a cause of an effect. In addition, existing model-based fault diagnosis methods may be able to identify the source of the fault, e.g., a valve leak. However, they cannot quantify the relative strengths of the different explanations (and diagnosis results). On the other hand, our method can quantify them, as already shown in Table 1 and 2. These, we believe, demonstrate the power of our method.

## VII. CONCLUSION

In order to explain to humans the anomalies occurring in CPSs so that FDD tasks can be performed with human advantages, this paper proposed a temporal logic called causal signal temporal logic. This logic has the ability to reason about the causation between a fault (cause) and the corresponding abnormal behaviors (effect). We also presented an algorithm for inferencing this logic based on a simulation model. The performance comparison with other formal interpretation methods on our developed ECLSS Simulink model verifies the advantage of our method in quantifying causality. In the future, we will keep developing methodologies that combine the strengths of formal methods and causality theory for explainable anomaly response for CPSs.

## REFERENCES

- [1] R. V. Yohanandhan, R. M. Elavarasan, P. Manoharan, and L. Mihet-Popa, "Cyber-physical power system (CPPS): A review on modeling, simulation, and analysis with cyber security applications," *IEEE Access*, vol. 8, pp. 151019–151064, 2020.
- [2] S. Pasandideh, P. Pereira, and L. Gomes, "Cyber-physical-social systems: Taxonomy, challenges, and opportunities," *IEEE Access*, vol. 10, pp. 42404–42419, 2022.
- [3] E. A. Lee, "Cyber physical systems: Design challenges," in *Proc. 11th IEEE Int. Symp. Object Compon.-Oriented Real-Time Distrib. Comput. (ISORC)*, May 2008, pp. 363–369.
- [4] L. Hu, N. Xie, Z. Kuang, and K. Zhao, "Review of cyber-physical system architecture," in *Proc. IEEE 15th Int. Symp. Object/Compon./Service-Oriented Real-Time Distrib. Comput. Workshops*, Apr. 2012, pp. 25–30.
- [5] J.-R. Jiang, "An improved cyber-physical systems architecture for industry 4.0 smart factories," in *Proc. Int. Conf. Appl. Syst. Innov. (ICASI)*, May 2017, pp. 918–920.
- [6] A. Ahmadi, A. H. Sodhro, C. Cherifi, V. Cheutet, and Y. Ouzrout, "Evolution of 3C cyber-physical systems architecture for industry 4.0," in *Proc. Service Orientation Holonic Multi-Agent Manuf. (SOHOMA)*. Cham, Switzerland: Springer, 2019, pp. 448–459.
- [7] M. Sampayo and P. Peças, "CPSD2: A new approach for cyber-physical systems design and development," *J. Ind. Inf. Integr.*, vol. 28, Jul. 2022, Art. no. 100348.
- [8] M. A. R. Garcia, R. Rojas, L. Gualtieri, E. Rauch, and D. Matt, "A human-in-the-loop cyber-physical system for collaborative assembly in smart manufacturing," *Proc. CIRP*, vol. 81, pp. 600–605, Jan. 2019.
- [9] X. Xuan, X. Zhang, O.-H. Kwon, and K.-L. Ma, "VAC-CNN: A visual analytics system for comparative studies of deep convolutional neural networks," *IEEE Trans. Vis. Comput. Graphics*, vol. 28, no. 6, pp. 2326–2337, Jun. 2022.
- [10] B. Wang, H. Zhou, G. Yang, X. Li, and H. Yang, "Human digital twin (HDT) driven human-cyber-physical systems: Key technologies and applications," *Chin. J. Mech. Eng.*, vol. 35, no. 1, p. 11, Dec. 2022.
- [11] H. Liu and L. Wang, "Remote human-robot collaboration: A cyber-physical system application for hazard manufacturing environment," *J. Manuf. Syst.*, vol. 54, pp. 24–34, Jan. 2020.
- [12] J. Boi-Ukeme, C. Ruiz-Martin, and G. Wainer, "Real-time fault detection and diagnosis of CPS faults in DEVS," in *Proc. IEEE 6th Int. Conf. Dependability Sensor, Cloud Big Data Syst. Appl. (DependSys)*, Dec. 2020, pp. 57–64.
- [13] C. Alippi, S. Ntalampiras, and M. Roveri, "Model-free fault detection and isolation in large-scale cyber-physical systems," *IEEE Trans. Emerg. Topics Comput. Intell.*, vol. 1, no. 1, pp. 61–71, Feb. 2017.
- [14] L. Piardi, P. Costa, A. Oliveira, and P. Leitão, "Collaborative fault detection and diagnosis architecture for industrial cyber-physical systems," in *Proc. IEEE Int. Conf. Ind. Technol. (ICIT)*, Aug. 2022, pp. 1–6.
- [15] S.-C. Wu and A. H. Vera, "Capability considerations for enhancing safety on long duration crewed missions: Insights from a technical interchange meeting on autonomous crew operations," *J. Space Saf. Eng.*, vol. 7, no. 1, pp. 78–82, Mar. 2020.
- [16] S. P. Eshima, J. Nabity, and R. Moroshima, "Analysis of fault propagation of environmental control and life support system for self-awareness," in *Proc. ASCEND*, 2020, p. 4012.
- [17] C. Baier, C. Dubslaff, F. Funke, S. Jantsch, R. Majumdar, J. Piribauer, and R. Ziemek, "From verification to causality-based explanations," in *Proc. 48th Int. Colloq. Automata, Lang., Program. (ICALP)*, vol. 198. Wadern, Germany: Schloss Dagstuhl-LeibnizZentrum für Informatik, 2021, pp. 1–20.
- [18] C. Baier and J.-P. Katoen, *Principles of Model Checking*. Cambridge, MA, USA: MIT Press, 2008.
- [19] Z. Kong, A. Jones, and C. Belta, "Temporal logics for learning and detection of anomalous behavior," *IEEE Trans. Autom. Control*, vol. 62, no. 3, pp. 1210–1222, Mar. 2017.
- [20] E. Bartocci, N. Manjunath, L. Mariani, C. Mateis, and D. Ničković, "CPS-Debug: Automatic failure explanation in CPS models," *Int. J. Softw. Tools Technol. Transf.*, vol. 23, no. 5, pp. 783–796, Oct. 2021.
- [21] G. Bombara and C. Belta, "Offline and online learning of signal temporal logic formulae using decision trees," *ACM Trans. Cyber-Physical Syst.*, vol. 5, no. 3, pp. 1–23, Jul. 2021.
- [22] Z. Deng and Z. Kong, "Interpretable fault diagnosis for cyberphysical systems: A learning perspective," *Computer*, vol. 54, no. 9, pp. 30–38, Sep. 2021.
- [23] J. Pearl, *Causality*. Cambridge, U.K.: Cambridge Univ. Press, 2009.
- [24] S. Kleinberg, "A logic for causal inference in time series with discrete and continuous variables," in *Proc. 22nd Int. Joint Conf. Artif. Intell.*, Jun. 2011, pp. 943–950.
- [25] J. Y. Halpern, *Actual Causality*. Cambridge, MA, USA: MIT Press, 2016.
- [26] T. Miller, "Explanation in artificial intelligence: Insights from the social sciences," *Artif. Intell.*, vol. 267, pp. 1–38, Feb. 2019.
- [27] G. Manco, E. Ritacco, P. Rullo, L. Gallucci, W. Astill, D. Kimber, and M. Antonelli, "Fault detection and explanation through big data analysis on sensor streams," *Exp. Syst. Appl.*, vol. 87, pp. 141–156, Nov. 2017.
- [28] E. Eells, *Probabilistic Causality*, vol. 1. Cambridge, U.K.: Cambridge Univ. Press, 1991.
- [29] A. Rashid and O. Hasan, "Formal analysis of the continuous dynamics of cyber-physical systems using theorem proving," *J. Syst. Archit.*, vol. 112, Jan. 2021, Art. no. 101850.

- [30] J. Runge, S. Bathiany, E. Bollt, G. Camps-Valls, D. Coumou, E. Deyle, C. Glymour, M. Kretschmer, M. D. Mahecha, J. Muñoz-Marí, and E. H. Van Nes, "Inferring causation from time series in earth system sciences," *Nature Commun.*, vol. 10, no. 1, p. 2553, Jun. 2019.
- [31] J. M. Mooij, D. Janzing, and B. Schölkopf, "From ordinary differential equations to structural causal models: The deterministic case," in *Proc. 29th Conf. Uncertainty Artif. Intell.*, 2013, pp. 440–448.
- [32] A. Donzé, "On signal temporal logic," in *Proc. Int. Conf. Runtime Verification*. Cham, Switzerland: Springer, 2013, pp. 382–383.
- [33] A. Donzé and O. Maler, "Robust satisfaction of temporal logic over real-valued signals," in *Proc. Int. Conf. Formal Model. Anal. Timed Syst.* Cham, Switzerland: Springer, 2010, pp. 92–106.
- [34] N. Mehdipour, C.-I. Vasile, and C. Belta, "Arithmetic-geometric mean robustness for control from signal temporal logic specifications," in *Proc. Amer. Control Conf. (ACC)*, Jul. 2019, pp. 1690–1695.
- [35] V. Raman, A. Donzé, M. Maasoumy, R. M. Murray, A. Sangiovanni-Vincentelli, and S. A. Seshia, "Model predictive control with signal temporal logic specifications," in *Proc. 53rd IEEE Conf. Decis. Control*, Dec. 2014, pp. 81–87.
- [36] P. I. Frazier, "Bayesian optimization," in *Recent Advances in Optimization And Modeling of Contemporary Problems*. New York, NY, USA: Inform, 2018, pp. 255–278.
- [37] M. Seeger, "Gaussian processes for machine learning," *Int. J. Neural Syst.*, vol. 14, no. 2, pp. 69–106, 2004.
- [38] N. Srinivas, A. Krause, S. M. Kakade, and M. W. Seeger, "Information-theoretic regret bounds for Gaussian process optimization in the bandit setting," *IEEE Trans. Inf. Theory*, vol. 58, no. 5, pp. 3250–3265, May 2012.
- [39] L.-M. Wang and Y.-M. Shao, "Crack fault classification for planetary gearbox based on feature selection technique and K-means clustering method," *Chin. J. Mech. Eng.*, vol. 31, no. 1, pp. 1–11, Dec. 2018.



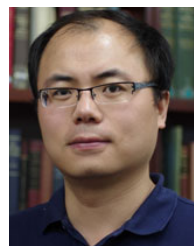
**ZIQUAN DENG** (Graduate Student Member, IEEE) received the bachelor's and master's degrees in mechanical engineering and aerospace engineering from Harbin Institute of Technology, Harbin, China, in 2016 and 2018, respectively, the master's degree in mechanical engineering from Washington University in St. Louis, St. Louis, MO, USA, in 2020. He is currently pursuing the Ph.D. degree with the Department of Mechanical and Aerospace Engineering, University of California at Davis, Davis, CA, USA. His research interests include formal methods and explainable cyber-physical systems/artificial intelligence.



**SAMUEL P. ESHIMA** received the bachelor's degree in mechanical engineering from Kanazawa University, in 2018, and the master's degree in aerospace engineering sciences from the University of Colorado, Boulder, CO, USA, in 2020, where he is currently pursuing Ph.D. degree with the Department of Smead Aerospace Engineering Sciences. His research interest includes sensor suite optimization for ECLSS anomaly detection and diagnostics.



**JAMES NABILITY** received the Ph.D. degree in mechanical engineering from the University of Colorado (CU), Boulder, CO, USA, in 2007. He is currently an Associate Professor with the Smead Aerospace Engineering Sciences Department, with a research focus on bioastronautics—the study and support of life in space. His current research advances environmental control and life support (ECLS) technologies with a focus on ionic liquid membranes for atmosphere revitalization and CO<sub>2</sub> capture, the use of ionic liquid solvents to extract minerals and oxygen from regolith, explore the effects of space radiation on habitat layout and crew performance, develop bioregenerative systems, and investigate heat transport and fluid flow in microgravity. Prior to joining CU in 2013, he was a Principal Engineer of TDA research, and before that, he was an Engineer with the Naval Air Warfare Center (NAWC) advancing the development of propulsion systems, burners and combustors, and ECLS technologies for spacecraft and submarines. He is a NAWC Technical Fellow (1996) for contributions to combustion, an AIAA Associate Fellow (2016), and the AIAA Life Sciences and Systems Technical Program Chair for the International Conference on Environmental Systems.



**ZHAODAN KONG** (Member, IEEE) received the bachelor's and master's degrees in astronautics and mechanics from Harbin Institute of Technology, Harbin, China, in 2004 and 2006, respectively, and the Ph.D. degree in aerospace engineering with a minor in cognitive science from the University of Minnesota, Twin Cities, MN, USA, in 2011. He is currently an Associate Professor in mechanical and aerospace engineering with the University of California at Davis (UC Davis), Davis, CA, USA. His current research interests include control theory, machine learning, formal methods, applications to human-machine systems, cyber-physical systems, and neural engineering. Before joining UC Davis in 2015, he was a Postdoctoral Researcher with the Laboratory for Intelligent Mechatronic Systems and the Hybrid and Networked Systems Laboratory, Boston University, Boston, MA, USA.

...